EXPLOSION PROPAGATION OF NON-HOMOGENEOUS METHANE–AIR CLOUDS INSIDE AN OBSTRUCTED 50 m³ VENTED VESSEL

B.H. HJERTAGER, M. BJØRKHAUG and K. FUHRE

Chr. Michelsen Institute, Dept. of Science and Technology, N-5036 Fantoft, Bergen (Norway)

(Received January 21, 1988; accepted in revised form April 25, 1988)

Summary

An experimental study of flame and pressure development of non-homogeneous methane clouds has been performed in a large scale obstructed tube of diameter 2.5 m and length 10 m and with one end closed and the other end open. The non-homogeneous clouds were generated by injecting the methane through various types of leak arrangements. Two types of leakages were simulated, namely guillotine breaks in pipes (axial leaks) and gasket failures in flanges (radial leaks). Three different leakage cross-sectional areas were tested. Prior to ignition several gas samples were withdrawn from the tube to establish the gas cloud inhomogeneity inside the tube. The results indicate that the explosion pressure produced is highly dependent on leak parameters such as leak arrangement, mass of fuel injected and ignition delay time. Explosion pressures may reach values as high as in the corresponding tests using homogeneous methane clouds. This was found for all the axial jet leaks tested (diameters 2, 5 and 8 cm) with a mass injected equal to the stoichiometric mass and using ignition delay times smaller than about 15 seconds. The radial leaks, using stoichiometric mass, produced smaller pressures than the corresponding axial leaks.

1. Introduction

In an industrial plant located either on-shore or off-shore the following hazard situation could occur. Flammable gases are released due to a gasket leak, a pipe rupture or even a vessel rupture. During and after the release the flammable gas will entrain air and form an explosive gas cloud. An accidental gas explosion may occur if this explosive gas cloud reaches an ignition source. The resultant outcome of such an explosion scenario, with regard to the pressure load produced, is particularly dependent on cloud type, size and location; and the obstacle and venting arrangement of the surrounding volume.

Previous works [1–7] have mainly focused attention on the influence of the distribution and shape of obstructions on the explosion pressures produced. The clouds were, in all these tests, stoichiometric and homogeneous throughout the vessel volume. Tests using homogeneous clouds of varying concentration have been conducted by Hjertager et al. [8]. The results of these studies

showed that there was a marked effect of concentration on the pressure build-up. The maximum was found at slightly rich mixtures for both methane/air and propane/air mixtures. Further it was found that the limits to flame propagation were somewhat narrower than the standard flammability limits.

The studies mentioned above are of course idealized situations when compared to an industrial situation. This is especially true for the homogeneous cloud assumption. The question then arises: to what extent does the non-homogeneity of a real gas cloud modify the conclusions reached in the previous studies?
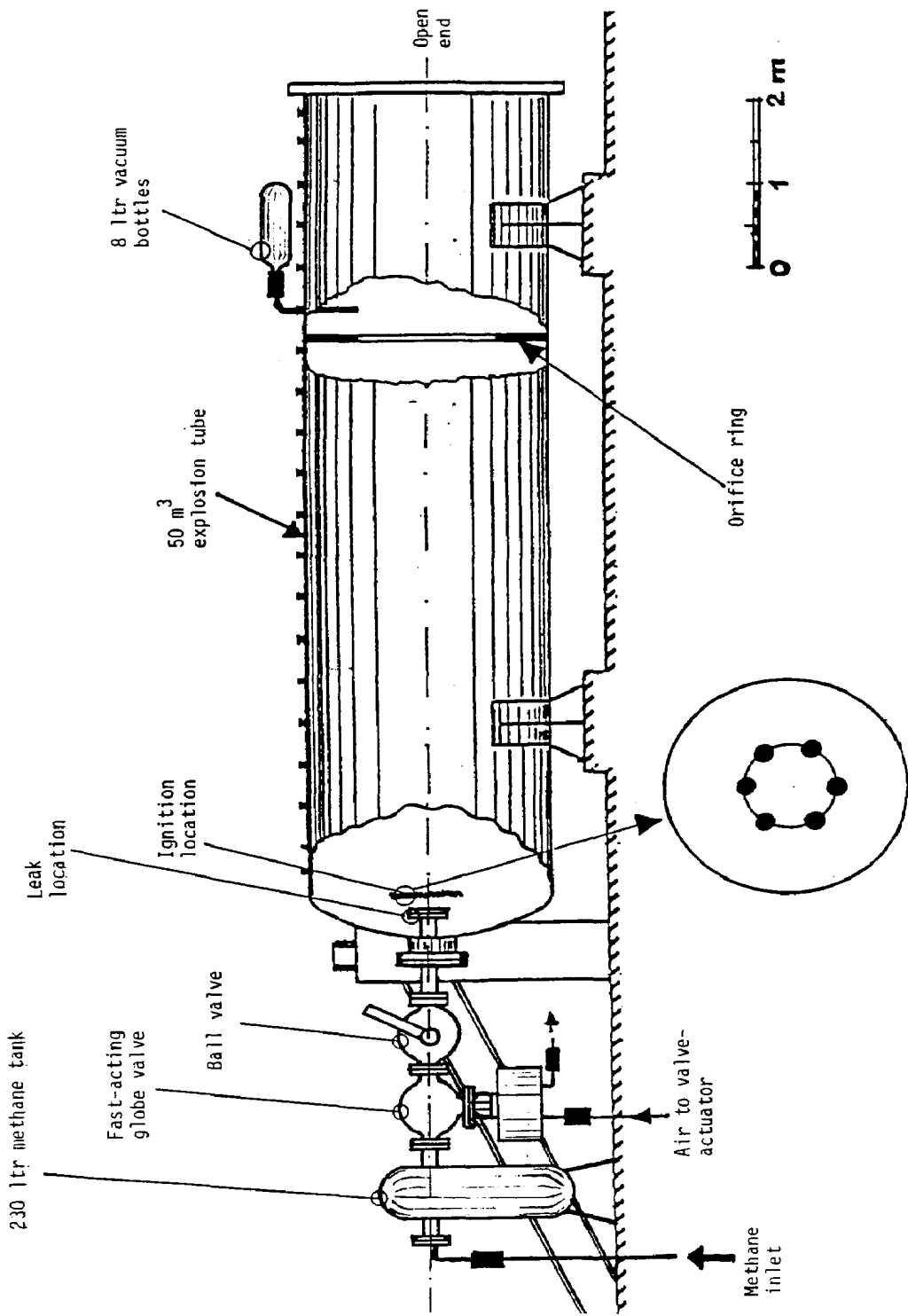
An experimental test series described in this report was undertaken to obtain some key data on non-homogeneous methane–air explosions in large-scale situations. In order to get direct comparison with previous results [8], the tests were performed in the 50 m³ combustion tube using the same obstacle arrangement as well as mass of fuel as given by Hjertager et al. [8]. The only new aspect introduced was the non-homogeneous methane–air clouds. To create non-homogeneous clouds, several new parameters are, however, introduced, being related to the leak source. Based on practical experience three different leak sizes, namely small, medium and large leak rates were chosen. In addition, two leak arrangements were used, namely axial and radial leaks. These arrangements could simulate full guillotine breaks in pipelines and gasket failures in flanges, respectively.

The present paper will give the results of the explosion tests using non-homogeneous methane–air clouds. The tests were performed on a test site at Sund on the island of Sotra, close to Bergen.

2. Experimental arrangements

The combustion tube used in these experiments had a diameter of 2.5 m and was 10 m long. One end of the tube was fully open and the other end was closed by a shell equipped with a flanged 0.46 m diameter opening. The leak generation arrangement was connected to the flange at the closed end of the combustion tube. The schematic tube facility is shown in Fig. 1. The ignition source was placed close to the leak source and consisted of six equally spaced match heads (ICI Ce-Mg) mounted on a 1 m diameter ring (see Fig. 1). This ignition mode is similar to the point ignition used in Ref. 8.

Preparation of the required mass of methane was accomplished by filling the 230 litre tank with pure methane to a predetermined pressure level. The tank was designed so that the stoichiometric mass of 3.2 kg methane was obtained by filling the tank to an overpressure of 20 bar. This methane mass, homogeneously distributed inside the 50 m³ tube, would have the stoichiometric concentration of 9.5 vol. % methane in air. Other methane masses could be prepared by filling the methane tank to different pressure levels. For example, a tank overpressure of 10 bar would be equivalent to half the stoichiometric mass and

Fig. 1. Schematic diagram of explosion tube facility.

a) Axial leaks

Methane from tank

Combustion tube wall

Direction of leak

Inner diameter 4 inches (100 mm)

Diameters, d = 20, 50 or 80 mm

b) Radial leaks

c) Gasket leaks

t' = 1 mm

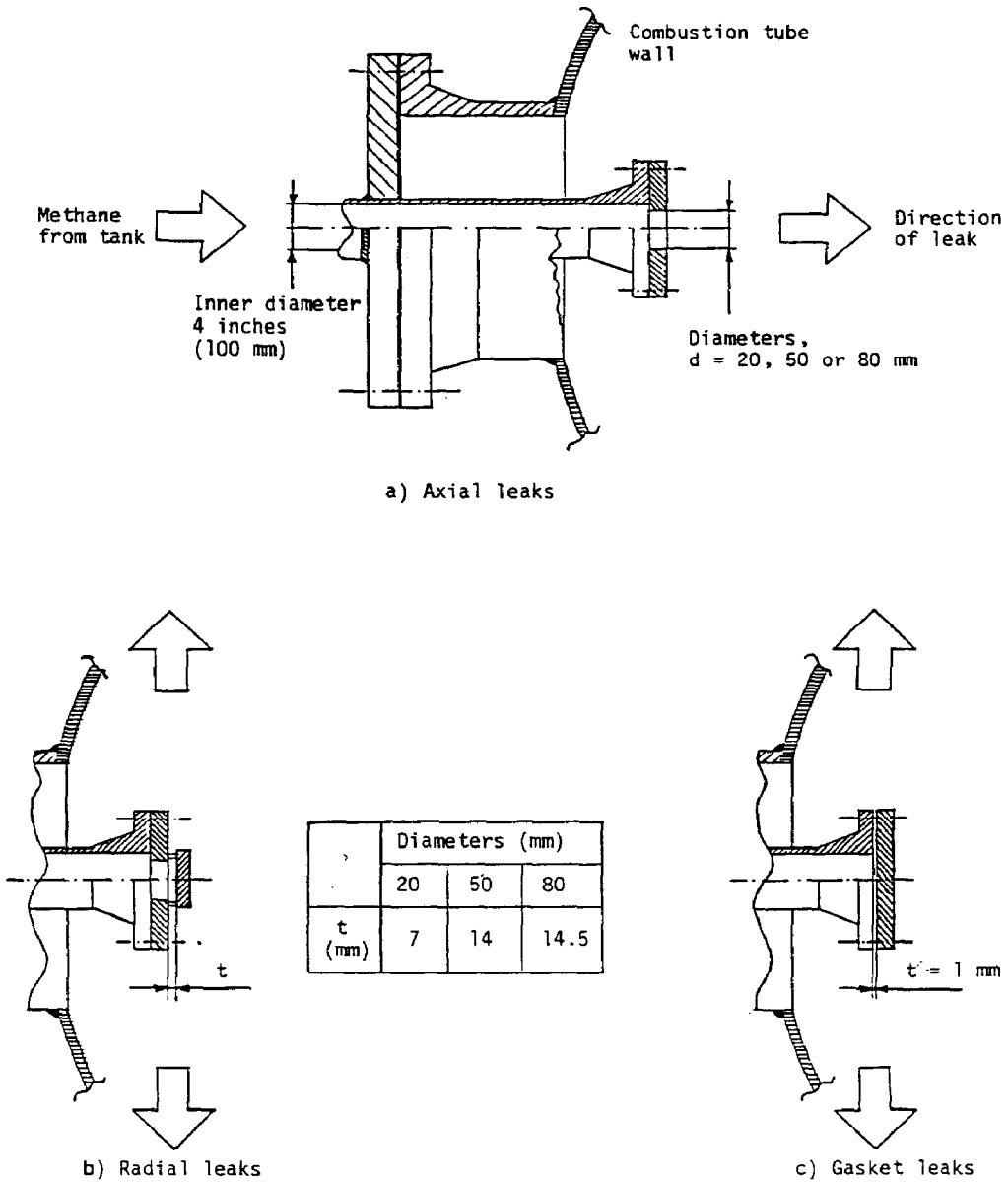|	Diameters (mm)		
	20	50	80
t (mm)	7	14	14.5

Fig. 2a–c. Schematic diagram showing the layouts of the three leak situations tested.

30 bar would be equivalent to one and half times the stoichiometric mass. The homogeneous equivalent concentrations for these methane masses would then be 4.75 vol. % and 14.25 vol. % respectively. During filling of the methane tank both the fast-acting globe valve and the ball valve were closed. When the desired tank pressure was reached the ball valve was opened manually. The leak

TABLE 1

Leak flowrates

Initial tank pressure (bar)	Initial leak flow rates (kg/s)			Methane mass (kg)
	Leak area (cm^2)/leak diameter (cm)			
	3.14/2	19.6/5	50.3/8	
10	0.46	3.18	8.17	1.6
20	0.97	6.1	15.6	3.2
30	1.44	8.97	23.0	4.8

was initiated by remotely opening the fast-acting globe valve. The methane was then allowed to flow through a 100 mm diameter pipe towards the leak arangement placed inside the combustion tube. Details of the three different leak arrangements used are given in Fig. 2, namely axial, radial and gasket arrangements. For the first two leak arrangements three different leak areas were tested. These were 3.14 cm^2, 19.6 cm^2 and 50.3 cm^2. Table 1 summarizes the initial leak flow-rates based on the three different methane masses and the three different leak areas tested.

For the gasket leak arrangement given in Fig. 2c only one leak area was tested, namely 3.14 cm^2. As shown in the figure, this indicated a 1 mm radial slot in a 4 inch (100 mm) diameter pipe. After the methane mass had been injected through the leak into the combustion tube the ignition was initiated following a certain predetermined ignition delay. Zero delay time was defined when the tank overpressure had decreased to 0.5 bar. The various ignition delays used varied from 0 seconds up to 90 seconds. Just prior to ignition, gas samples of the explosive mixture were withdrawn from different places inside the combustion tube by the use of several 8 litre vacuum bottles. These samples were analyzed after each explosion test by using an infrared gas analyzer (Binos 1, Leybold and Heraeus). These measurements could then be used to establish the methane concentration of the explosive cloud just prior to ignition. In contrast to the previous test series [5] no plastic sheet covered the tube outlet.

Synchronisation of the ignition delay, operation of the gas sampling bottles, resetting, and calibration of the pressure transducers were controlled by a 10-channel programmed timer (UP timer, Xanadu Controls). The signals were recorded on a 14 channel analog tape recorder (PR 2230, Ampex Corporation). After each test the records were displayed with a multichannel UV-recorder (Autograph 8, Bryans). Four types of diagnostic probes were used to monitor the explosion event. Concentrations prior to ignition were monitored at up to twelve different locations along the tube centre-line, as well as along the shear layers of the ring obstacles. The flame position inside the tube was recorded
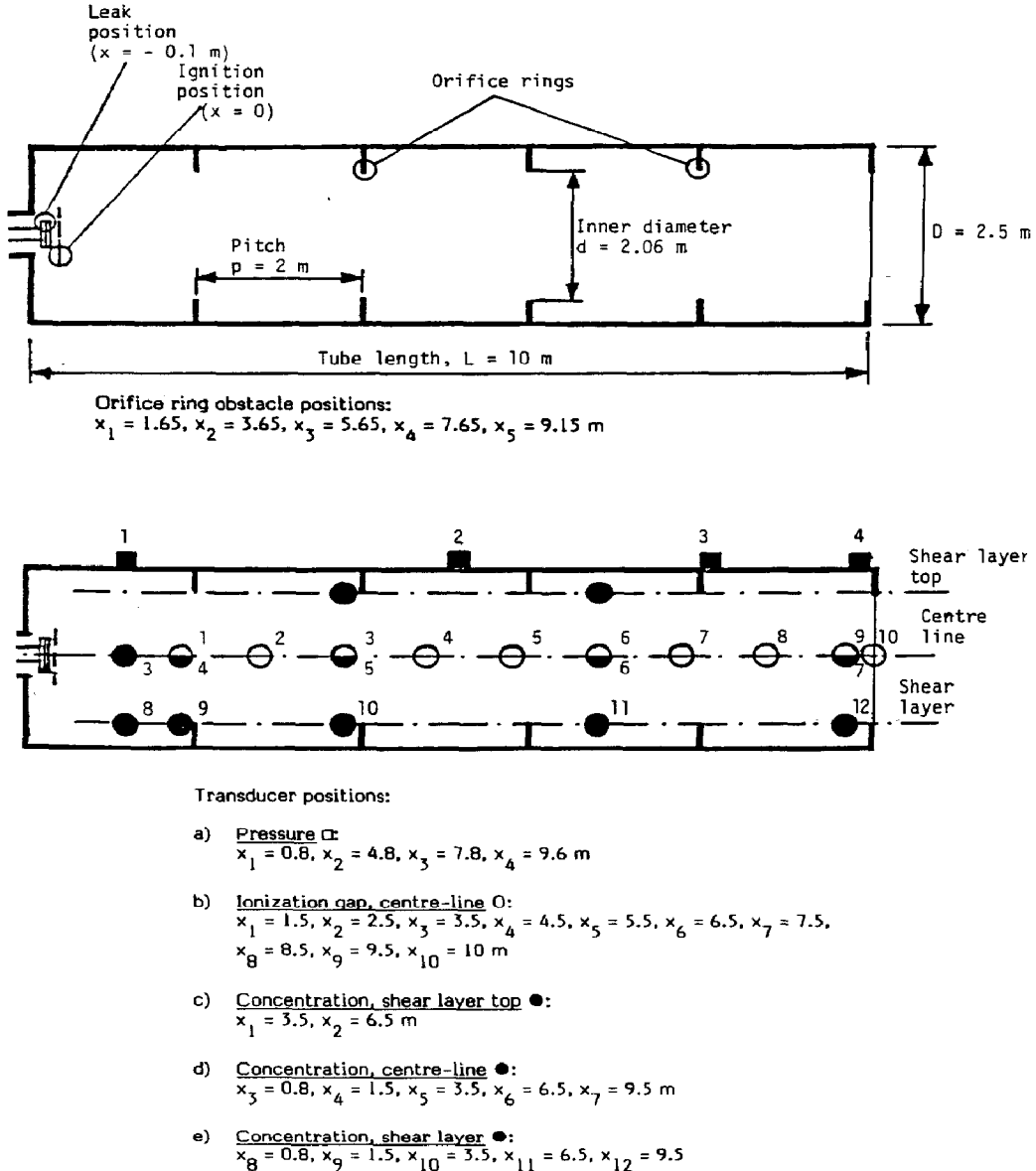
Fig. 3. Schematic diagram showing the obstacle configuration and diagnostic probe positions.

by using ten regularly-spaced ionization gap probes mounted on a rod placed along the tube centre-line. The inside pressure was measured by four pressure transducers (603B, Kistler) mounted at various positions along the tube wall. The outside blast wave was monitored by a transducer (LC 33, Celesco) placed

10 m from the tube exit at an angle of approximately 10° from the tube axis. The details of the probe positions are given in Fig. 3.

154 explosion tests were performed for one obstacle configuration inside the tube. The obstacles consisted of five steel rings with outside diameter equal to the combustion tube diameter ($D = 2.5$ m) and inside diameter (d) was 2.06 m. The rings were regularly positioned along the tube and provided a fixed blockage ratio, $BR = 1 - (d/D)^2 = 0.3$, to the flow. The geometry schematically shown in Fig. 3 is the same as that used by Hjertager et al. [8] in their homogeneous gas cloud tests.

3. Results and discussion

3.1 General

The results of the tests showed a strong influence of the leak parameters on the resulting explosion pressure load. The largest peak pressure measured at the tube outlet amounted to approximately 3.5 bar. This was found for a 2 cm axial leak situation with a mass of methane equal to stoichiometric and an ignition delay time of 5 seconds. The radial leaks produced smaller pressure than the axial ones and the maximum pressure produced for a radial situation was approximately 1 bar. This was found for 1 mm gasket leak, using a mass of fuel equal to 50% of the stoichiometric mass. The ignition delay time for this test was 0 seconds after injection of the methane mass. In addition to these maximum loads, pressures could attain any value between zero and the maximum, dependent on the ignition delay.

In order to put these results into some perspective in relation to the homogeneous cloud tests performed by Hjertager et al. [8] using both planar and point source ignition, comparisons are shown in Figs. 4 and 5. In these figures we have chosen to show the peak pressures produced for all the axial (Fig. 4) and radial (Fig. 5) tests using the largest leak diameter of 8 cm. The abcissa is the homogeneous concentration of methane in air and for the non-homogeneous tests we plot the results according to the equivalent concentration based on the injected methane mass and volume of tube. In Fig. 4 we can see that peak pressures as high as the point source ignited homogeneous clouds are obtained for the stoichiometric mass. However, this fuel mass also produces pressures that may be lower. For the two other methane masses, namely 50% stoichiometric and 150% stoichiometric, the maximum pressures are smaller than for the stoichiometric case, but larger than the homogeneous cases.

The 8 cm radial leak results are shown in Fig. 5. Here we observe that the stoichiometric mass produces maximum pressures that are much smaller than the homogeneous point-ignited case, but the 50% stoichiometric case produces maximum pressures that are larger than the corresponding axial leak case. The 150% stoichiometric case, on the other hand, produces smaller pressures than the axial case. Although the results in Figs. 4 and 5 are for the largest leak area,
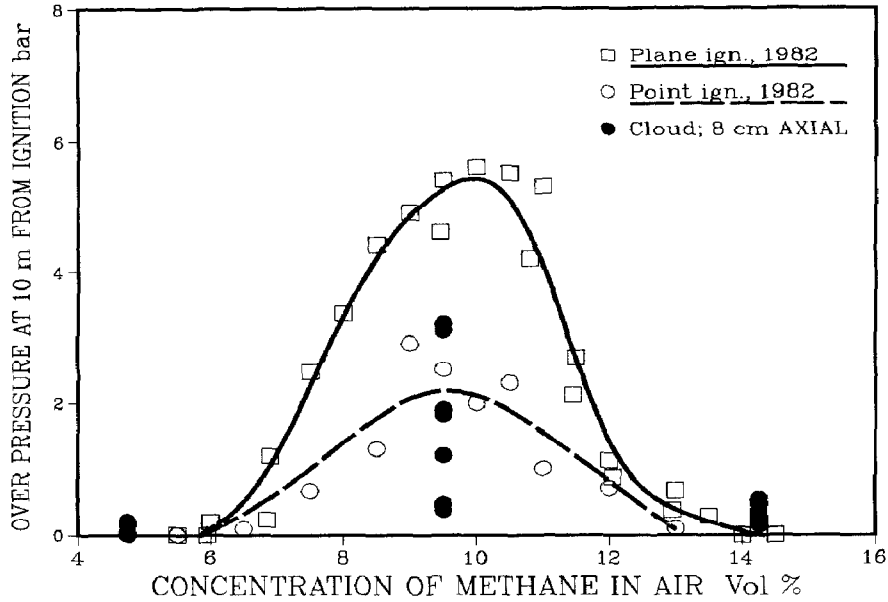
Fig. 4. Peak overpressure as a function of methane concentration for point and planar ignited homogeneous clouds as well as non-homogeneous clouds. Axial leaks. 8 cm.
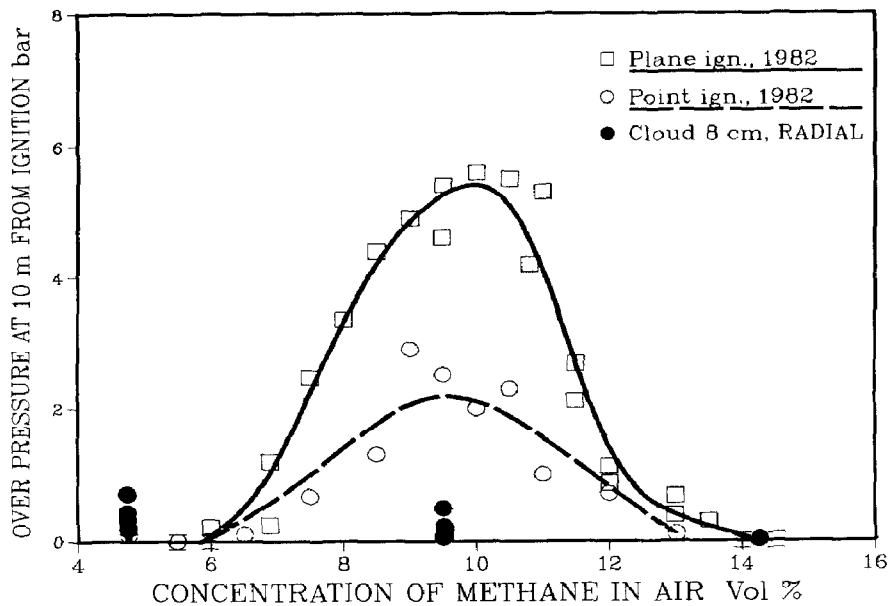

Fig. 5. Peak overpressure as a function of methane concentration for point and planar ignited homogeneous clouds as well as non-homogeneous clouds. Radial leaks. 8 cm.
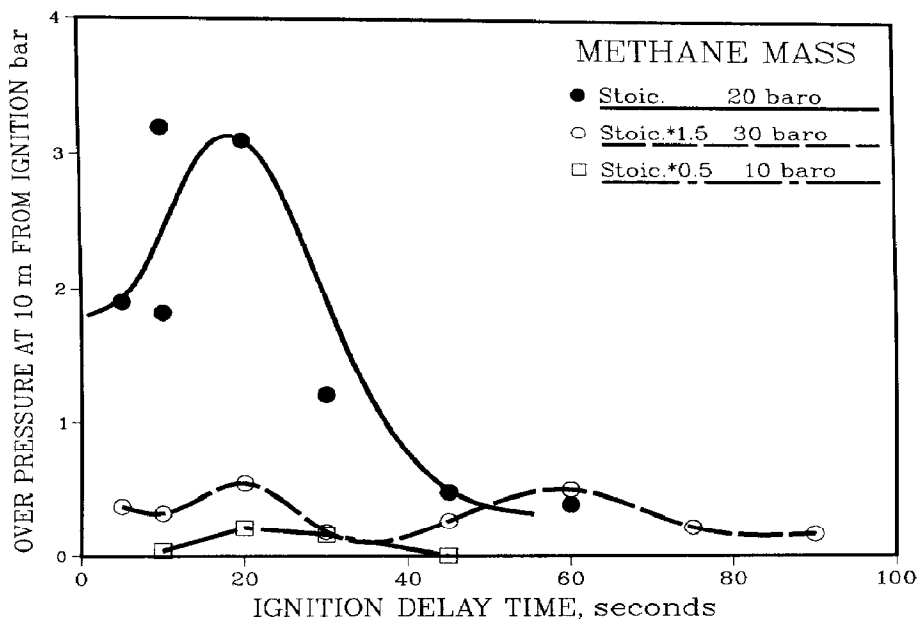
Fig. 6. Peak overpressure as a function of ignition delay time for 8 cm axial leak.
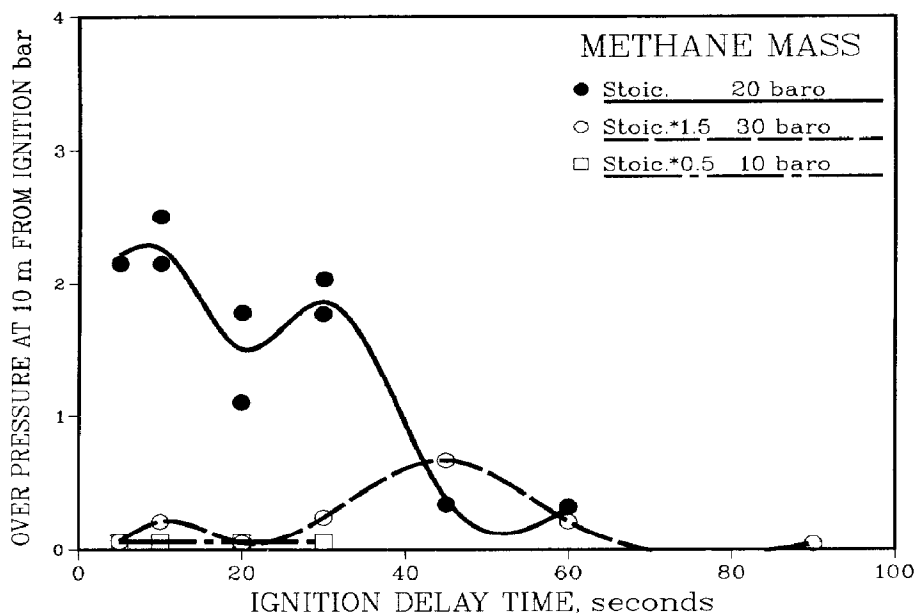

Fig. 7. Peak overpressure as a function of ignition delay time for 5 cm axial leak.

similar results are also found for the two smaller leak areas tested. It should therefore be obvious that the non-homogeneity in methane concentration may obtain pressures that are as high as or even higher than the corresponding
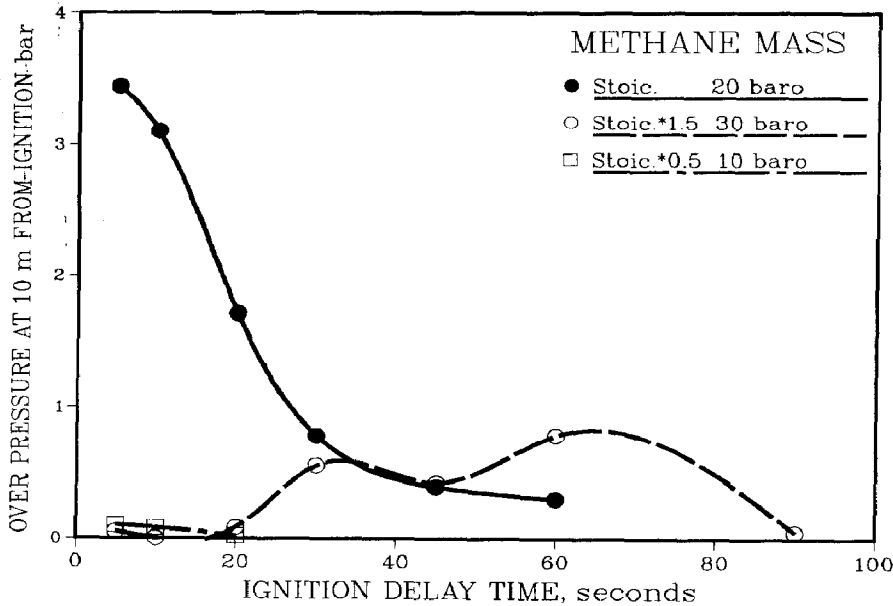
Fig. 8. Peak overpressure as function of ignition delay time for a 2 cm axial leak.

homogeneous clouds. But these maxima are only obtained when certain conditions are met. In our case this is related to ignition delay time and layout of leak source.

3.2 Axial leaks

Figures 6–8 show the explosion pressure results from the axial leaks for different ignition delay times. The results show that the largest pressures for the stoichiometric mass are obtained for ignition delay times smaller than approximately 50 seconds. It is also seen that for the 50% stoichiometric mass cases, much lower peak pressures are measured in comparison with the stoichiometric mass. The 150% stoichiometric mass tests also show smaller pressure build-up than the stoichiometric ones, but larger pressures than the 50% stoichiometric mass. The largest methane mass maintains the pressures for longer ignition delay times as compared with the other two masses.

The concentration data for the axial jet cases show that the concentration is fairly constant over the cross sections along the tube for small ignition delay times. For larger delay times stratification due to buoyancy plays a larger role and gives rise to higher methane concentrations along the top of the tube. This is of course due to the fact that methane is lighter than air. For all the 150% stoichiometric mass cases shown in Figs. 6 to 8, a second peak appears in the pressure produced versus ignition delay times. Detailed study of the concentration data explains this. For these large mass cases buoyancy is more important than for the smaller masses. More methane generates more buoyancy and
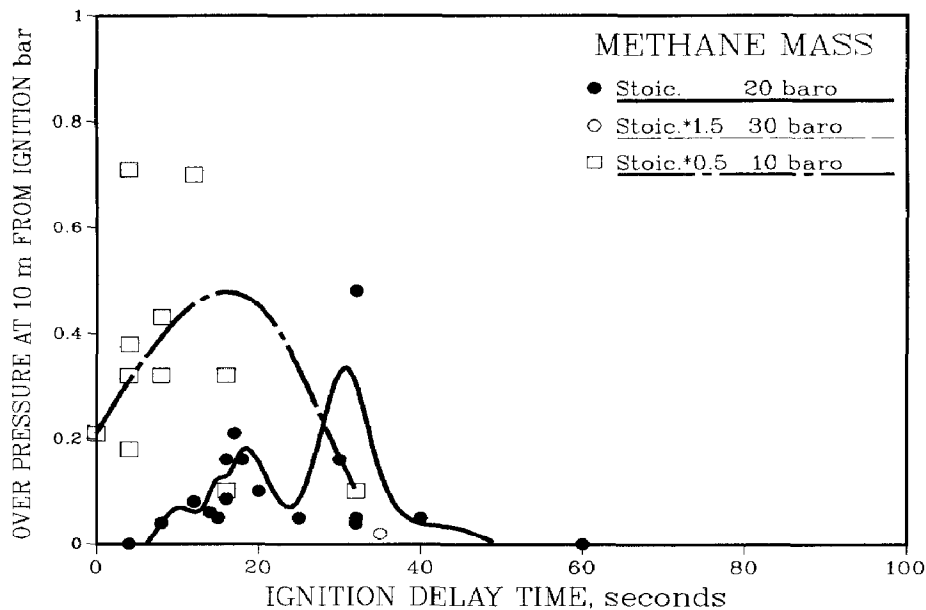
Fig. 9. Peak overpressure as a function of ignition delay time for 8 cm radial leak.
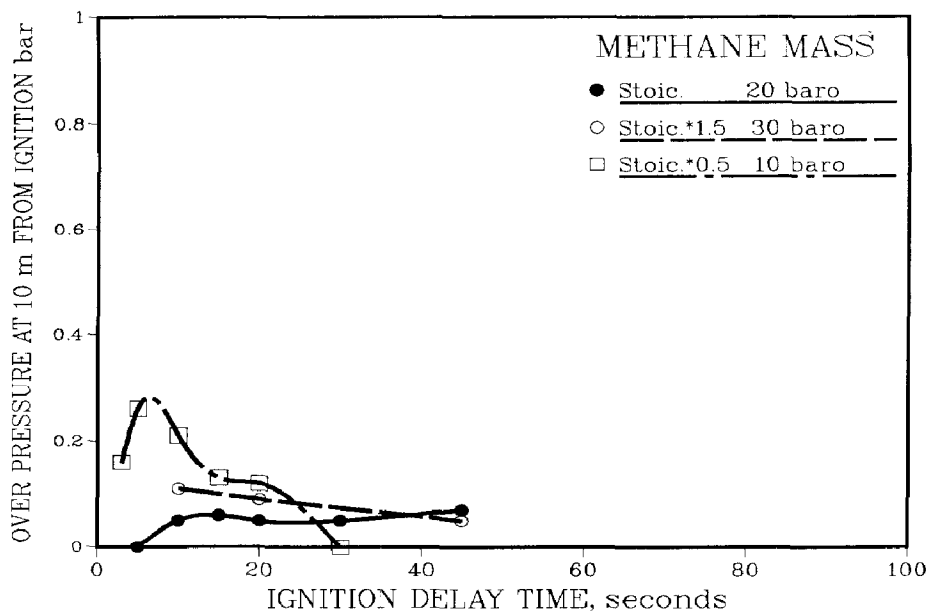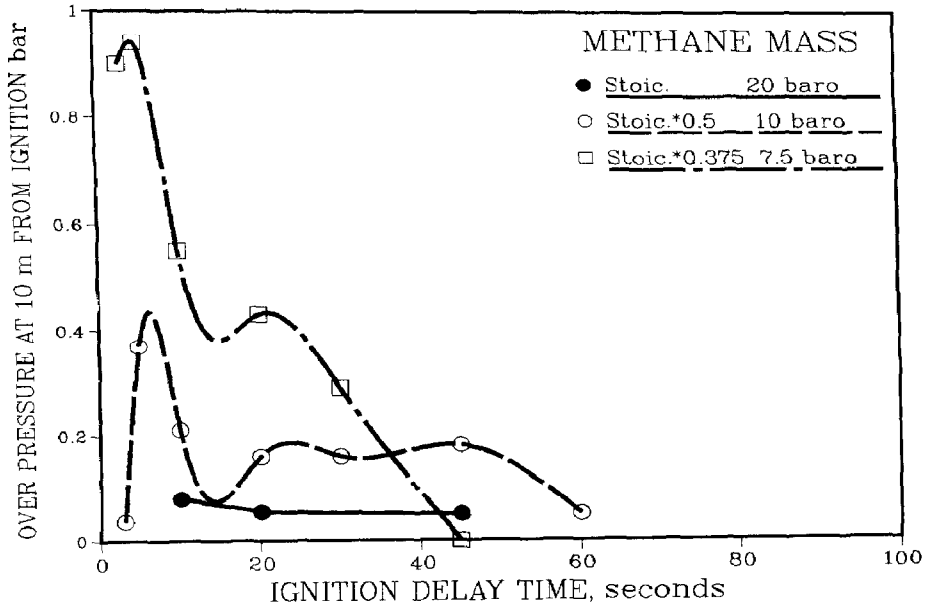

Fig. 10. Peak overpressure as function of ignition delay time for 5 cm radial leak.

more methane also needs more time to get downmixed to optimum concentration (~ 10% methane in air). Hence, the appearance of the second peak for this methane mass situation.

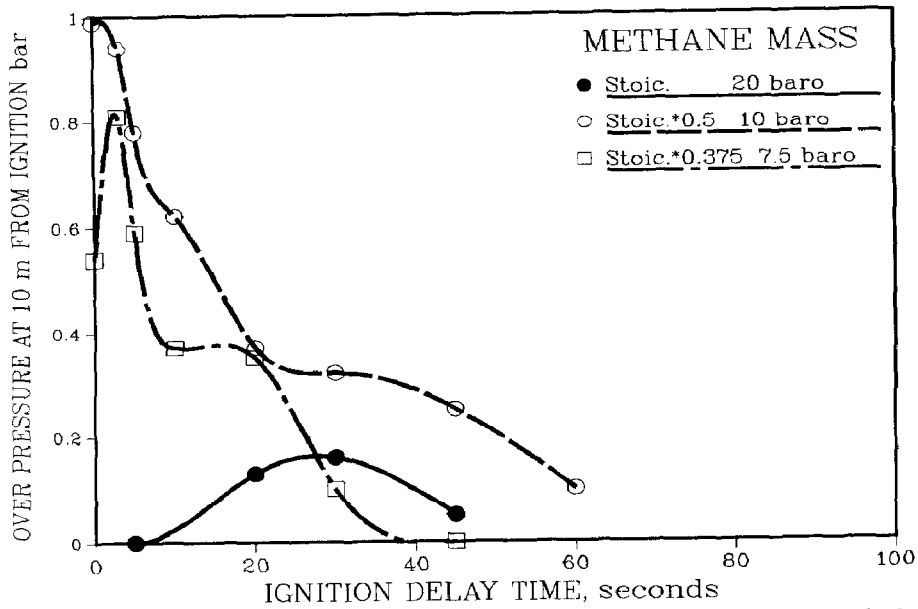Fig. 11. Peak overpressure as a function of ignition delay time for 2 cm radial leak.

Fig. 12. Peak overpressure as function of ignition delay time for 1 mm gasket leak in 4 inch (100 mm) flange.
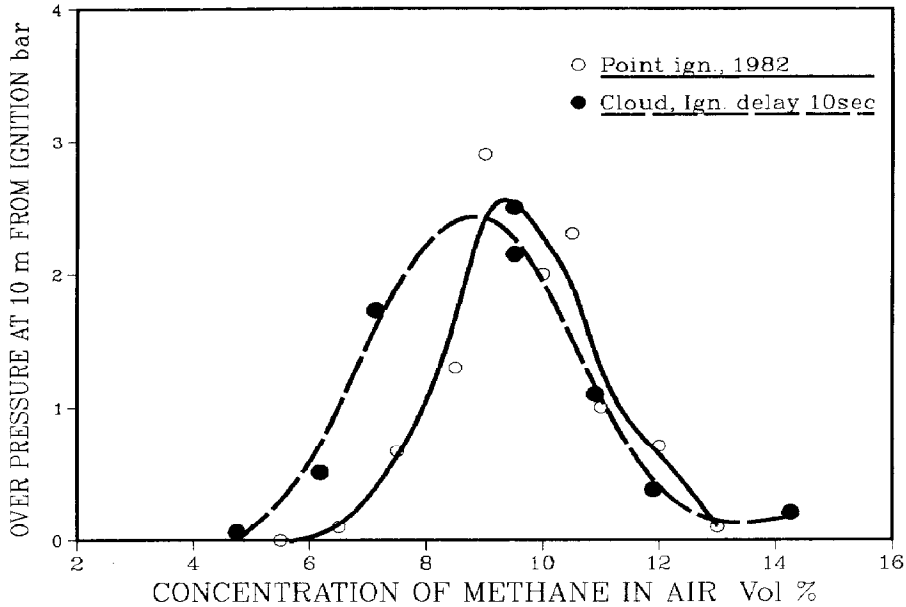
Fig. 13. Peak overpressure as a function of homogeneous concentration for 5 cm axial leak with constant ignition delay, 10 seconds.
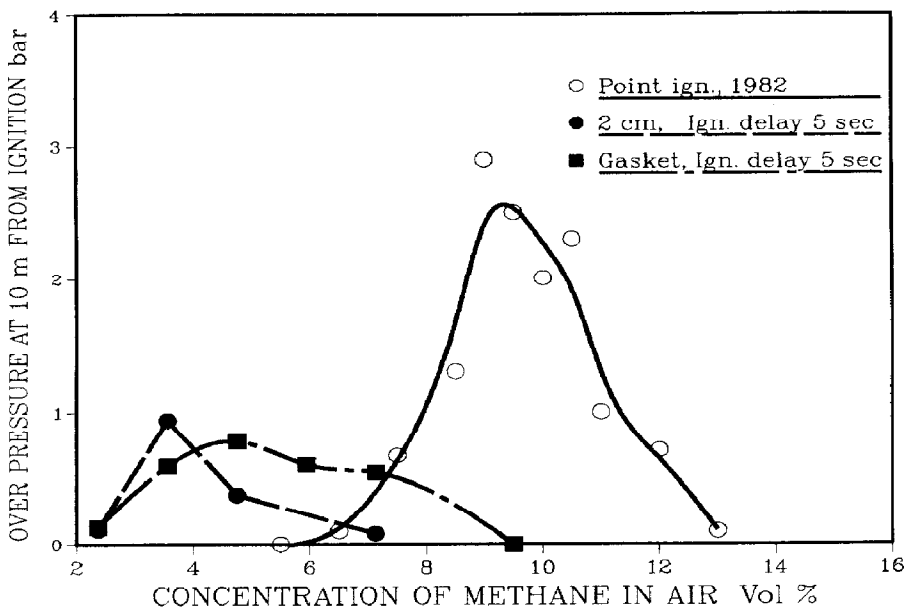

Fig. 14. Peak overpressure as a function of homogeneous concentration for 2 cm radial and 1 mm gasket leak with constant ignition delay, 5 seconds.

3.3 Radial leaks

Figs. 9–12 show the explosion pressure results from the radial leaks and gasket leaks for different ignition delay times. The results show that the largest pressures are found for methane masses that are smaller than the stoichiometric one. For these smaller masses the pressure produced generally decays with increasing ignition delay time. For the stoichiometric masses, however, there is a tendency towards a delayed maximum. This may, as for the axial leak tests, also be related to the increased time needed to get downmixed to the optimum concentrations for faster flame propagation. It is seen from examination of the detailed concentration data that, for all of the radial leaks, a very inhomogeneous cloud is formed. The methane penetrates towards the walls close to the leak end of the tube, leaving the last part of the tube with a low methane concentration. The axial leak could penetrate much further towards the end of the tube in comparison with the radial leak. This then explains the reason for optimum pressure build-up for the smaller methane masses in the radial leak cases as compared to the axial ones.

3.4 Further discussion

Figures 13 and 14 show comparisons between homogeneous clouds and the axial and radial leaks for fixed ignition delay times. These figures again display the general differences between the axial, radial and homogeneous methane cloud explosions.

It has become apparent from the present tests that the pressure loads produced may attain values that are as high as the corresponding homogeneous cloud tests. It has also been found that the non-homogeneity may, for smaller methane masses, produce explosion pressures that are higher than for the homogeneous clouds. In hazard analysis, this indicates that the homogeneous stoichiometric cloud case could be seen upon as a credible upper limit even for non-homogeneous clouds. It has also become evident that the leak flow area is not a decisive parameter. The three most important leak parameters seem to be the fuel mass ejected, the leak arrangement and the ignition delay.

4. Conclusions

1. Non-homogeneous methane–air clouds may produce pressures that are as high as the corresponding homogeneous cloud cases. This is, however, only obtained when certain conditions are met.
2. Largest explosion pressures are obtained for axial leak arrangements with mass equivalent to the stoichiometric ones and ignition delays smaller than 50 seconds. For radial leak arrangements peak explosion pressures are found for methane masses smaller than stoichiometric.
3. The most important leak parameters turned out to be: (i) the mass of fuel

ejected, (ii) the leak arrangement and, (iii) the ignition delay. The leak area turned out to have a small influence on the explosion pressures produced.

4. The present study indicates that the stoichiometric homogeneous cloud assumption constitutes a credible upper limit scenario for use in hazard analysis even though the cloud may be non-homogeneous.

Acknowledgements

References

1 R.K. Eckhoff, K. Fuhre, C.M. Guirao and J.H.S. Lee, Venting of turbulent gas explosions in a 50 m^3 chamber, Fire Saf. J., 7 (1984) 191–197.
2 I.O. Moen, J.H.S. Lee, B.H. Hjertager, K. Fuhre and R.K. Eckhoff, Pressure development due to turbulent flame propagation in large-scale methane–air explosions, Combustion and Flame, 47 (1982) 31–52.
3 B.H. Hjertager, K. Fuhre, S.J. Parker and J.R. Bakke, Flame acceleration of propane–air in a large-scale obstructed tube, 9th International Colloquium on Dynamics of Explosions and Reactive Systems, Poitiers, France, 3–8 July 1983. Prog. Am. Inst. Aeronaut. Astronaut., Vol. 94, pp. 504–522, 1984.
4 M. Bjørkhaug and B.H. Hjertager, The influence of obstacles on flame propagation and pressure development in a radial vessel of ten metre radius, Chr. Michelsen Institute, CMI Report No. 843403–9, 1984.
5 I.O. Moen, M. Donato, R. Knystatas and J.H.S. Lee, Flame acceleration due to turbulence produced by obstacles, Combustion and Flame, 39 (1980) 31–32.
6 P.A. Urtiew, J. Brandeis and W.J. Hogan, Experimental study of flame propagation in semiconfined geometries with obstacles, Combust. Sci. Technol., 30 (1983) 105–119.
7 C.J.M. van Wingerden and J.P. Zeeuwen, Flame propagation in the presence of repeated obstacles: influence of gas reactivity and degree of confinement, J. Hazardous Materials, 8 (1983) 139–156.
8 B.H. Hjertager, K. Fuhre and M. Bjørkhaug, Concentration effects on flame acceleration by obstacles in large-scale methane–air and propane–air explosions, Submitted for publication in Combust. Sci. Technol., 1988.